ACS OMEGA

http://pubs.acs.org/journal/acsodf

Article

Cycloartane- and Lanostane-Type Triterpenoids from the Resin of *Parthenium argentatum* AZ-2, a Byproduct of Guayule Rubber Production

Ya-ming Xu, Chandrashekhar Madasu, Manping X. Liu, E. M. Kithsiri Wijeratne, David Dierig, Bob White, István Molnár, and A. A. Leslie Gunatilaka*

Cite This: *ACS Omega* 2021, 6, 15486−15498

Read Online

ACCESS | Metrics & More | Article Recommendations | Supporting Information

ABSTRACT: A total of 12 new cycloartane- and lanostane-type triterpenoids including 16-deoxyargentatin A (**1**), 16-deoxyisoargentatin A (**2**), 7-oxoisoargentatin A (**3**), 24-*epi*-argentatin H (**4**), 24-*O*-*p*-anisoylargentatin C (**5**), 24-*O*-*trans*-cinnamoylargentatin C (**6**), 16-dehydroargentatin C (**7**), 16,17(20)-didehydroargentatin C (**8**), isoargentatin C (**9**), isoargentatin H (**10**), 3-*epi*-quisquagenin (**11**), and isoquisquagenin (**12**) together with 10 known triterpenoids (**13**−**22**) were isolated from the resin of *Parthenium argentatum* AZ-2 obtained as a byproduct of Bridgestone guayule rubber production. The structures of new triterpenoids **1**−**12** and argentatin H (**13**), which has previously been characterized as its diacetate (**23**), were elucidated by extensive analysis of their spectroscopic data and chemical conversions, and the known compounds **14**−**22** were identified by comparison of their spectroscopic data with those reported. Of these, **13**, **14**, and **18** exhibited weak cytotoxic activity for several cancer cell lines.

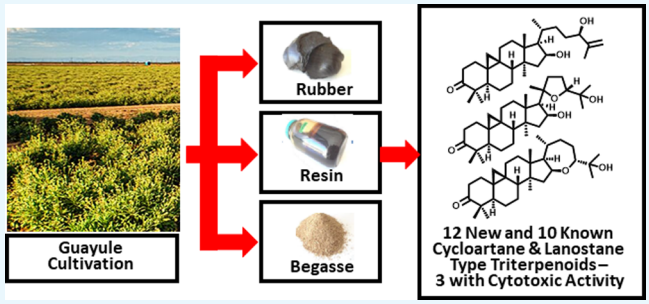

INTRODUCTION

Guayule (*Parthenium argentatum* A. Gray, Asteraceae), a plant native to the southwestern United States and the Chihuahuan desert of northern Mexico,[1] is currently undergoing economic assessment as a reliable and sustainable source of natural rubber.[2] The outcome of this evaluation will determine the suitability of this plant as a commercially viable crop for arid land agriculture. Commercial processing of guayule for rubber involves extraction of the dried and chopped plant biomass with an acetone−hexane azeotrope, which results in an equal or larger amount of guayule resin,[3] a byproduct with no current cost-effective commercial applications. It has been suggested that finding and/or developing high-value resin-based products could significantly ameliorate the manufacturing cost of guayule rubber.[4] Previous studies on *P. argentatum* resin have resulted in the isolation of some major constituents including the cycloartane-type triterpenoids, argentatins A−C,[5] and the sesquiterpenoids, guayulins A−D,[6] whereas lanostane-type triterpenoids isoargentatins A and B, together with argentatins A−D, have been encountered in the roots of *P. argentatum*.[7] Investigation of the resin of the hybrid plant, *P. argentatum* × *Parthenium tomentosum*, has afforded two pyridine alkaloids, guayulamines A and B,[9] in addition to argentatins E−H, of which argentatins G and H were characterized as their diacetates.[8] In addition to argentatins and guayulins, several fatty acid triglycerides have been isolated and characterized from the resins of some cultivars of *P. argentatum*.[10]

Guayule resin and some of its constituents are known to exhibit a variety of biological activities. The ability of guayule resin to protect wood from termite attack has been reported,[11] and subsequent studies have demonstrated moderate termite antifeedant activity of argentatin B.[12] Several argentatins have been reported to exhibit weak cytotoxic[13] and antimicrobial activities.[14] Importantly, despite its weak *in vitro* cytotoxic activity, argentatin A has recently been demonstrated to have promising *in vivo* antitumor activity in a mouse xenograft model of human colon cancer at high doses with no adverse toxicity.[15]

In our attempts to develop value-added products as a part of a collaborative USDA/NIFA-funded project on Sustainable Bio-economy for Arid Regions, we initiated a study to identify constituents of guayule resin with potential biological activity and/or those constituents which can be converted into their bioactive analogues. Herein, we report a detailed chemical

Received: April 20, 2021
Accepted: May 21, 2021
Published: June 4, 2021

investigation of resin samples obtained during guayule rubber processing by Bridgestone Americas Inc., which led to the isolation and characterization of 12 new and 10 known cycloartane- and lanostane-type triterpenoids, and evaluation of their cytotoxic activity.

MATERIALS AND METHODS

General Experimental Procedures. Optical rotations were measured with a JASCO Dip-370 polarimeter using MeOH as the solvent. UV spectra were recorded with a Shimadzu UV 2601 spectrophotometer. Electronic circular dichroism (ECD) spectra were measured with a JASCO J-810 spectropolarimeter. One-dimensional (1D) and two-dimensional (2D) NMR spectra were recorded in $CDCl_3$ using the residual solvent as the internal standard on a Bruker AVANCE III 400 spectrometer at 400 MHz for ^1H NMR and 100 MHz for ^{13}C NMR, respectively. The chemical shift values (δ) are given in parts per million (ppm), and the coupling constants (J values) are in Hz. Low-resolution MS spectra were recorded on a Thermo LQX mass spectrometer and high-resolution MS spectra on an Agilent G6224A TOF mass spectrometer. Analytical thin-layer chromatography (TLC) was carried out on silica gel 60 F_{254} aluminum-backed TLC plates (Merck), and preparative TLC was performed on Analtech silica gel 500 μm glass plates. Compounds were visualized with short-wavelength UV (254 nm) and by spraying with anisaldehyde-sulfuric acid reagent and heating until the spots appeared. Silica gel flash chromatography was accomplished using 230−400 mesh silica gel. Sephadex LH-20 for gel-permeation chromatography was obtained from Amersham Biosciences. HPLC purifications were carried out using a Phenomenex Luna 5 μm C_{18} (2) column (10 × 250 mm) for RP-C_{18} chromatography and Econosil Si (10 μ) column (10 × 250 mm) for NP chromatography with a Waters Delta Prep system containing a PDA 996 detector. When required, MM2 energy minimizations of all possible conformers were carried out using Chem3D 15.0 from PerkinElmer, Inc. The resin samples (ID 2017-7-1-Res-45 and ID 2018-1-1-Res-25) extracted from *P. argentatum* line AZ-2[16] used in this study were from the Bridgestone Americas Biorubber Process Research Center, Mesa, Arizona.

Isolation and Purification of Guayule Resin Constituents. Guayule resin (Bridgestone ID 2017-7-1-Res-45, 1.43 g) was first fractionated by solvent−solvent partitioning with 80% aq MeOH (100 mL) and hexanes (3 × 30 mL). The 80% aq MeOH fraction thus obtained was diluted with water to make it to 50% aq MeOH, which was then extracted with $CHCl_3$ (3 × 80 mL). Evaporation of each of these afforded hexanes (844 mg), $CHCl_3$ (570 mg), and 50% aq MeOH (5.6 mg) fractions. The hexanes fraction (844 mg) was further fractionated by gel-permeation chromatography on a column of Sephadex LH-20 (100 g). Elution with CH_2Cl_2/hexanes (4:1) afforded five fractions A1−A5. Of these, the major fraction A2 (288 mg) was subjected to silica gel (100 g) column chromatography and eluted with $CHCl_3$ to afford **18** (30.0 mg) and several minor fractions, which were further purified by RP-C_{18} HPLC using aq. MeOH [gradient ranging from 85% MeOH−90% MeOH in H_2O to yield **1** (2.5 mg), **2** (1.0 mg), **13** (13.0 mg), **16** (9.1 mg), **19** (7.2 mg), and **21** (0.9 mg)]. The $CHCl_3$ fraction (570 mg) obtained from the above solvent−solvent partitioning was subjected to gel-permeation chromatography on Sephadex LH-20 (100 g). Elution with CH_2Cl_2/hexanes (4:1, v/v) afforded 10 fractions [B1 (61 mg), B2 (109 mg), B3 (210 mg), B4 (32 mg), B5 (98 mg), B6 (10 mg), B7 (31 mg), B8 (9 mg), B9 (25 mg), and B10 (42 mg)]. Of these, the major fractions with clear spots by TLC were further fractionated. Purification of fraction B2 (109 mg) by silica gel (100 g) column chromatography and elution with $CHCl_3$/MeOH (98:2, v/v) gave **18** (35.0 mg). Fraction B3 (210 mg) on further fractionation by silica gel (100 g) column chromatography and elution with $CHCl_3$/MeOH (98:2, v/v) afforded **14** (112.8 mg) and fractions containing several minor constituents which were further purified by RP-C_{18} HPLC. Elution with a gradient of 85−95% aq MeOH (v/v) afforded **3** (1.5 mg), **5** (0.9 mg), **6** (1.0 mg), **8** (2.1 mg), **9** (2.1 mg), **15** (4.1 mg), **19** (3.6 mg), and **20** (2.3 mg). Fraction B5 (50.0 mg) was further purified by silica gel (50 g) column chromatography, and elution with $CHCl_3$/MeOH (98:2, v/v) afforded **13** (8.0 mg) and **16** (12.5 mg).

A second sample of the resin (Bridgestone ID 2018-1-1-Res-25, 116.0 g) was subjected to silica gel (3.5 kg) column chromatography. Elution with a solvent gradient of hexanes, hexanes/EtOAc (95:5 to 50:50, v/v), and EtOAc afforded 12 fractions [C1 (7.2 g), C2 (11.0 g), C3 (13.0 g), C4 (7.4 g), C5 (2.0 g), C6 (13.7 g), C7 (4.9 g), C8 (28.0 g), C9 (4.5 g), C10 (7.6 g), C11 (6.5 g), and C12 (10.0 g)]. Of these, only the fractions suspected to contain triterpenoids by TLC were further investigated. Fraction C4 (7.4 g) which contained a major compound when washed with hexanes (× 3) removed colored impurities, yielding **18** (6.18 g). A portion of the fraction C6 (2.0 g) was subjected to silica gel (60.0 g) column chromatography and eluted with CH_2Cl_2/acetone (98:2 to 90:10, v/v) to afford eight subfractions (C6-1 to C6-8). Further fractionation of C6-6 (400 mg) by silica gel (12 g) column chromatography and elution with CH_2Cl_2/acetone (99:1, v/v) yielded **19** (110 mg). Subfraction C6-7 (150 mg) was subjected to gel permeation chromatography on Sephadex LH-20 (4.5 g). Elution with hexanes/CH_2Cl_2 (1:1, v/v) afforded **4** (5.0 mg). Fraction C7 (4.9 g) was further fractionated by silica gel (150 g) column chromatography, and elution with CH_2Cl_2/acetone (98:2 to 90:10, v/v) gave nine subfractions [C7-1 (172 mg), C7-2 (430 mg), C7-3 (1.5 g), C7-4 (920 mg), C7-5 (165 mg), C7-6 (139 mg), C7-7 (344 mg), C7-8 (756 mg), and C7-9 (268 mg)]. A portion of the fraction C7-5 (15.0 mg) was separated by RP-C_{18} HPLC with MeOH/H_2O (85:15, v/v, 3.0 mL/min) as the eluent to afford **10** (6.7 mg) and **13** (6.2 mg). Fraction C8 (28.0 g) was subjected to silica gel (900 g) column chromatography and elution with hexanes/EtOAc (98:2 to 0:100, v/v) gave **14** (8.0 g). Fraction C9 (3.3 g) was subjected to silica gel (100 g) column chromatography and eluted with CH_2Cl_2/*i*-PrOH (100:0 to 90:10, v/v) to afford seven subfractions [C9-1 (754 mg), C9-2 (500 mg), C9-3 (607 mg), C9-4 (280 mg), C9-5 (432 mg), C9-6 (570 mg), and C9-7 (190 mg)]. A portion of the fraction C9-4 (33.0 mg) was purified by RP-C_{18} HPLC with MeOH/H_2O (85:15, v/v, 3.0 mL/min) as the eluent to afford, **11** (13.0 mg), **12** (2.0 mg), and **15** (16.0 mg).

Fraction C10 (7.3 g) on silica gel (220 g) column chromatography and elution with a gradient of CH_2Cl_2/*iso*-PrOH (98:1 to 90:10, v/v) afforded nine subfractions [C10-1 (1.0 g), C10-2 (1.8 g), C10-3 (818 mg), C10-4 (328 mg), C10-5 (1.2 g), C10-6 (550 mg), C10-7 (190 mg), C10-8 (543 mg), and C10-9 (656 mg)]. Of these, subfraction C10-5 (1.2 g) which was suspected to contain triterpenes was further fractionated on a column of RP-C_{18} silica gel (36 g) and by elution with MeOH/H_2O (70:30 to 100:0, v/v) to provide **17**

https://doi.org/10.1021/acsomega.1c01714
ACS Omega 2021, 6, 15486−15498

Table 1. ^{1}H and ^{13}C NMR Data of 1−3 in $CDCl_3$

	1		2		3	
position	δ_H	δ_C	δ_H	δ_C	δ_H	δ_C
1	1.82 (m)	33.4 CH_2	1.63 (m)	36.0 CH_2	2.40−2.50 (m)	34.2 CH_2
	1.52 (m)					
2	2.69 (dt, 6.5, 13.8)	37.5 CH_2	2.57 (m)	34.6 CH_2	2.97−3.05 (m)	35.1 CH_2
	2.28 (ddd, 2.6, 4.2, 13.8)		2.37 (m)			
3		216.7 C		217.9 C		218.2 C
4		50.2 C		47.4 C		47.1 C
5	1.68 (m)	48.5 CH	1.58 (m)	51.2 CH	1.65 (m)	51.6 CH
6	1.54 (m)	21.5 CH_2	1.59 (m)	19.4 CH_2	2.59−2.64 (m)	51.9 CH_2
	0.92 (m)		0.91 (m)			
7	2.05 (m)	25.9 CH_2	2.03 (m)	26.3 CH_2		198.4 C
	1.10 (m)		1.35 (m)			
8	1.58 (m)	47.6 CH		134.9 C		138.3 C
9		20.8 C		133.0 C		164.0 C
10		25.7 C		36.9 C		49.4 C
11	1.36 (m)	26.8 CH_2	2.02 (m)	21.1 CH_2	1.66 (m)	18.6 CH_2
	1.16 (m)				1.49 (m)	
12	1.65−1.76 (m)	33.1 CH_2	1.63−1.81 (m)	31.3 CH_2	2.38 (m)	29.2 CH_2
					2.28 (m)	
13		46.1 C		45.0 C		49.4 C
14		48.7 C		49.9 C		47.0 C
15	1.28−1.39 (m)	35.1 CH_2	1.22 (m)	30.5 CH_2	2.07 (m)	43.8 CH_2
					1.87 (m)	
16	1.63−1.79 (m)	25.1 CH_2	1.62−1.80 (m)	25.1 CH_2	4.68 (dd, 8.0, 13.6)	72.4 CH
17	2.11 (dd, 6.6, 9.7)	55.1 CH	2.00 (m)	53.3 CH	2.25 (m)	53.7 CH
18	1.14 (s)	19.8 CH_3	0.83 (s)	17.5 CH_3	1.23 (s)	19.9 CH_3
19	0.76 (d, 4.0)	29.8 CH_2	1.09 (s)	18.5 CH_3	1.08 (s)	27.3 CH_3
	0.56 (d, 4.0)					
20		84.9 C		85.0 C		86.4 C
21	1.22 (s)	26.1 CH_3	1.22 (s)	25.6 CH3	1.26 (s)	26.3 CH_3
22	1.83 (m)	38.4 CH2	1.79 (m)	38.2 CH2	2.20 (m)	37.3 CH_2
	1.58 (m)		1.56 (m)		1.71 (m)	
23	1.72−1.82 (m)	22.5 CH_2	1.72−1.87 (m)	22.5 CH_2	1.87−1.98 (m)	23.8 CH_2
24	3.75 (dd, 7.0, 8.2)	84.0 CH	3.74 (dd, 7.1, 7.9)	83.9 CH	3.82 (t, 8.0)	84.3 CH
25		71.7 C		71.7 C		70.9 C
26	1.21 (s)	27.5 CH_3	1.20 (s)	27.4 CH_3	1.23 (s)	27.4 CH_3
27	1.13 (s)	24.3 CH_3	1.12 (s)	24.3 CH_3	1.13 (s)	25.8 CH_3
28	1.03 (s)	22.2 CH_3	1.05 (s)	21.3 CH_3	1.11 (s)	20.6 CH_3
29	1.08 (s)	20.8 CH_3	1.07 (s)	26.1CH_3	1.06 (s)	27.7 CH_3
30	0.91 (s)	19.5 CH_3	0.90 (s)	24.5 CH_3	1.10 (s)	18.9 CH_3

(820 mg). Subfraction C10-2 (200 mg) on further purification by RP-C_{18} silica gel (6.0 g) column chromatography followed by RP-C_{18} HPLC and elution with MeOH/H_2O (80:20, v/v, 3.0 mL/min) afforded **7** (3.2 mg) and **8** (3.0 mg). Subfraction C10-8 (533 mg) was further fractionated on a column of RP-C_{18} silica gel (15 g) and by elution with MeOH/H_2O (70:30 to 100:0, v/v) to give four subfractions C10-8-1 (30.0 mg), C10-8-2 (11.0 mg), C10-8-3 (100 mg), and C10-8-4 (350 mg). Of these, C10-8-3 (24.5 mg) was separated by C_{18} RP HPLC with MeOH/H_2O (80:20, v/v, 3.0 mL/min) as the eluent to afford **22** (20.7 mg).

*16-Deoxyargentatin A [(20S,24R)-20,24-Epoxy-25-hydroxycycloartan-3-one] (**1**).* Amorphous colorless powder; $[\alpha]_D^{25}$ + 21.3 (*c* 0.24, MeOH); UV (MeOH) λ_{max}(log ε): 200 (3.43) nm; ECD (MeOH) [θ] −2059 (295 nm); ^{1}H and ^{13}C NMR data; see Table 1; positive HRESIMS *m*/*z* 439.3568 [MH − H_2O]$^+$ (calcd for $C_{30}H_{47}O_2$, 439.3571).

*16-Deoxyisoargentatin A [(20S,24R)-20,24-Epoxy-25-hydroxylanost-8-en-3-one] (**2**).* Amorphous colorless powder; $[\alpha]_D^{25}$ + 41.6 (*c* 0.09, MeOH); UV (MeOH) λ_{max} (log ε) 252 (3.28) nm; ECD (MeOH) [θ] −883 (252 nm), +991 (262 nm); ^{1}H and ^{13}C NMR data; see Table 1; positive HRESIMS *m*/*z* 439.3568 [MH − H_2O]$^+$ (calcd for $C_{30}H_{47}O_2$, 439.3571).

*7-Oxoisoargentatin A [(16β,20S,24R)-20,24-Epoxy-16,25-dihydroxylanost-8-en-3,7-dione] (**3**).* Amorphous colorless powder; $[\alpha]_D^{25}$ + 128.5 (*c* 0.14, MeOH); UV (MeOH) λ_{max} (log ε) 256 (3.72) nm; ECD (MeOH) [θ] −5597 (222 nm), +29,636 (256 nm), −5636 (341 nm); ^{1}H and ^{13}C NMR data; see Table 1; positive HRESIMS *m*/*z* 509.3256 [M + Na]$^+$ (calcd for $C_{30}H_{46}O_5Na$, 509.3238).

*24-Epi-argentatin H [(16β,20R,24S)-16,24-Dihydroxycycloart-25-en-3-one] (**4**).* Amorphous colorless powder; $[\alpha]_D^{25}$ + 52.0 (*c* 0.1, $CHCl_3$); UV (MeOH) λ_{max}(log ε) 276 (sh, 3.21) nm; ECD (MeOH) [θ] −1118 (297 nm); ^{1}H and ^{13}C NMR data; see Table 2; positive HRESIMS *m*/*z* 479.3490 [M + Na]$^+$ (calcd for $C_{30}H_{48}O_3Na$, 479.3496).

*24-O-p-Anisoylargentatin C [(16β,20R,24R)-24-p-Anisoyl-16,25-dihydroxycycloartan-3-one] (**5**).* Amorphous colorless

https://doi.org/10.1021/acsomega.1c01714
ACS Omega 2021, 6, 15486−15498

Table 2. ^{1}H and ^{13}C NMR Data of 4−7 in $CDCl_3$

	4		5		6		7	
position	δ_H	δ_C	δ_H	δ_C	δ_H	δ_C	δ_H	δ_C
1	1.82 (m)	33.4 CH_2	1.80 (m)	33.4 CH_2	1.84 (m)	33.4 CH_2	1.86 (m)	33.1 CH_2
	1.54 (m)		1.52 (m)		1.51 (m)		1.53 (m)	
2	2.69 (dt, 6.5, 13.6)	37.4 CH_2	2.68 (dt, 6.5, 13.6)	37.5 CH_2	2.70 (m)	37.5 CH_2	2.70 (dt, 6.3, 14.0)	37.3 CH_2
	2.28 (ddd, 2.6, 4.2, 14.0)		2.28 (ddd, 2.4, 4.2, 14.2)		2.28 (m)		2.31 (ddd, 2.6, 4.2, 14.0)	
3		216.5 C		216.5 C		216.6 C		216.0 C
4		50.2 C		50.2 C		50.2 C		50.2 C
5	1.68 (m)	48.4 CH	1.67 (m)	48.4 CH	1.68 (m)	48.4 CH	1.73 (dd, 4.4, 12.2)	48.3 CH
6	1.56 (m)	21.4 CH_2	1.54 (m)	21.4 CH_2	1.55 (m)	21.4 CH_2	1.59 (m)	20.8 CH_2
	0.95 (m)		0.93 (m		0.93 (m)		0.95 (m)	
7	1.37 (m)	26.1 CH_2	1.31 (m)	26.4 CH_2	1.31 (m)	26.4 CH_2	1.33 (m)	26.2 CH_2
	1.13 (m)		1.11 (m)		1.11 (m)		1.18 (m)	
8	1.63 (m)	47.8 CH	1.62 m)	47.9 CH	1.64 (m)	48.0 CH	1.65 (dd, 4.4, 12.4)	47.4 CH
9		20.8 C		20.9 C		20.9 C		20.3 C
10		25.9 C		26.1 C		26.0 C		26.4 C
11	2.04 (m)	26.4 CH_2	2.03 (m)	27.5 CH_2	2.03 (m)	27.4CH_2	2.15 (m)	26.2 CH_2
	1.20 (m)		1.11 (m)		1.10 (m)		1.23 (m)	
12	1.52−1.72 (m)	32.5 CH_2	1.53−1.67 (m)	32.6 CH_2	1.57−1.70 (m)	32.6 CH_2	1.95 (m)	32.1 CH_2
							1.23 (m)	
13		45.3 C		45.4 C		45.4 C		42.0 C
14		46.6 C		46.6 C		46.6 C		45.3 C
15	2.02 (m)	47.3 CH_2	1.96 (m)	48.0 CH_2	1.98 (m)	48.0 CH_2	2.05 (d, 18.7)	50.6 CH_2
	1.35 (m)		1.31 (m)		1.33 (m)		1.99 (d, 18.7)	
16	4.46 (dt, 5.2 7.5)	72.8 CH	4.27 (dt, 5.2, 7.8)	72.6 CH	4.35 (dt, 5.2, 7.8)	72.6 CH		221.3 C
17	1.63 (m)	56.8 CH	1.60 (m)	56.4 CH	1.64 (m)	56.4 CH	2.28 (d, 9.6)	62.0 CH
18	1.16 (s)	18.9 CH_3	1.12 (s)	19.0 CH3	1.14 (s)	19.0 CH3	1.12 (s)	18.7 CH_3
19	0.80 (d, 4.4)	29.8 CH_2	0.78 (d, 4.4)	29.9 CH2	0.79 (d, 4.4)	29.9 CH_2	0.83 (d, 4.4)	30.0 CH_2
	0.57 (d, 4.4)		0.56 (d, 4.4)		0.57 (d, 4.4)		0.63 (d, 4.4)	
20	1.63 (m)	27.2 CH	1.79 (m)	30.5 CH		30.5 CH	1.70 (m)	28.8 CH
21	0.93 (d, 6.2)	17.8 CH_3	0.94 (d, 6.4)	18.0 CH_3	0.95 (d, 6.4)	18.0 CH_3	0.95 (d, 6.6)	18.2 CH_3
22	1.79 (m)	30.8 CH2	2.02 (m)	26.4 CH_2	2.01 (m)	26.5 CH_2	1.96 (m)	32.1 CH2
	1.04 (m)		1.14 (m)		1.37 (m)		1.23 (m)	
23	1.49−1.73 (m)	30.6 CH_2	1.72−1.86 (m)	33.1 CH_2	1.58−1.70 (m)	33.0 CH_2	1.35−1.52 (m)	27.6 CH_2
24	4.20 (dd, 3.6, 10.0)	72.9 CH	4.95 (dd, 3.2, 9.0)	80.9 CH	4.87 (dd, 3.2, 8.6)	80.8 CH	3.50 (dt, 11.0, 2.8)	75.9 CH
25		147.9 C		72.9 C		72.7 C		72.6 C
26	4.98 (brs)	110.2 CH_2	1.26 (s)	25.6 CH_3	1.24 (s)	25.5 CH_3	1.20 (s)	26.5 CH_3
	4.80 (brs)							
27	1.71 (s)	18.2 CH_3	1.27 (s)	25.9 CH_3	1.24 (s)	25.9 CH_3	1.15 (s)	23.4 CH_3
28	1.08 (s)	20.8 CH_3	1.07 (s)	20.8 CH_3	1.07 (s)	20.8 CH_3	1.09 (s)	20.7 CH_3
29	1.02 (s)	22.1 CH_3	1.02 (s)	22.2 CH_3	1.02 (s)	22.1 CH_3	1.04 (s)	22.2 CH_3
30	0.87 (s)	19.9 CH_3	0.82 (s)	20.0 CH_3	0.84 (s)	20.0 CH_3	1.14 (s)	20.0 CH_3
1′				122.4 C		134.3 C		
2′/6′			7.99 (d, 8.8)	131.7 CH	7.52 (m)	128.2 CH		
3′/5′			6.91 (d, 8.8)	113.7 CH	7.38 (m)	128.9 CH		
4′				163.5 C	7.38 (m)	134.3 CH		
7′			3.85 (s)	55.5 CH_3	7.71 (d, 15.6)	145.6 CH		
8′				166.5 C	6.47 (d, 15.6)	117.8 CH		
9′						167.3 C		

powder; $[\alpha]_D^{25}$ + 6.6 (*c* 0.08, MeOH); UV (MeOH) λ_{max}(log ε) 256 (4.09) nm; ECD (MeOH) [θ] −5628 (260 nm); ^{1}H and ^{13}C NMR data; see Table 2; positive HRESIMS *m*/*z* 631.3989 $[M + Na]^+$ (calcd for $C_{38}H_{56}O_6Na$, 631.3970).

24-O-trans-Cinnamoylargentatin C [(16β,20R,24R)-24-trans-Cinnamoyl-16,25-dihydroxycycloartan-3-one] (**6**). Amorphous colorless powder; $[\alpha]_D^{25}$ + 15.5 (*c* 0.09, MeOH); UV (MeOH) λ_{max}(log ε) 275 (4.09) nm; ECD (MeOH) [θ] −4438 (281 nm); ^{1}H and ^{13}C NMR data; see Table 2; positive HRESIMS *m*/*z*: 627.4029 $[M + Na]^+$ (calcd for $C_{39}H_{56}O_5Na$, 627.4020).

16-Dehydroargentatin C [(20R,24R)-24,25-dihydroxycycloartan-3,16-dione] (**7**). Amorphous colorless powder; $[\alpha]_D^{25}$ − 79.5 (*c* 0.12, MeOH); UV (MeOH) λ_{max} (log ε) 260 (sh, 1.54) nm; ECD (MeOH) [θ] −28196 (301 nm); ^{1}H and ^{13}C NMR data; see Table 2; positive HRESIMS *m*/*z* 455.3509 $[MH - H_2O]^+$ (calcd for $C_{30}H_{47}O_3$, 455.3520).

16,17(20)-Didehydroargentatin C [(20R,24R)-24,25-Dihydroxycycloart-17-en-3,16-dione] (**8**). Amorphous colorless

https://doi.org/10.1021/acsomega.1c01714
ACS Omega 2021, 6, 15486−15498

Table 3. ^{1}H and ^{13}C NMR Data of 8−10 in $CDCl_3$

	8		9		10	
position	δ_H	δ_C	δ_H	δ_C	δ_H	δ_C
1	1.87 (m)	33.2 CH_2	1.96 (m)	35.9 CH_2	1.97 (m)	35.6 CH_2
	1.54 (m)		1.60 (m)		1.60 (m)	
2	2.71 (dt, 6.4, 14.0)	37.3 CH_2	2.57 (ddd, 7.1, 11.4, 15.8)	34.6 CH_2	2.57 (ddd, 7.1, 11.4, 15.8)	34.6 CH_2
	2.31 (ddd, 2.4, 4.0, 14.0)		2.38 (ddd, 3.6, 6.7, 15.8)		2.38 (ddd, 3.6, 6.7, 15.8)	
3		216.1C		217.8 C		217.7 C
4		50.2 C		47.4 C		47.4 C
5	1.72 (4.6, 12.2)	48.2 CH	1.58 (m)	51.2 CH	1.58 (m)	51.2 CH
6	1.60 (m)	21.2 CH_2	1.55−1.67 (m)	19.4 CH_2	1.54−1.66 (m)	19.3 CH_2
	0.96 (m)					
7	1.36 (m)	25.9 CH_2	2.04−2.16 (m)	26.2 CH_2	2.00−2.18 (m)	26.1 CH_2
	1.15 (m)					
8		45.6 CH		134.6 C		134.7 C
9		20.2 C		133.6 C		133.6 C
10		26.3 C		36.9 C		36.9 C
11	2.18 (m)	26.4 CH_2	1.95−2.07 (m)	20.7 CH_2	1.95−2.15 (m)	20.7 CH_2
	1.31 (m)					
12	2.08 (m)	30.8 CH_2	1.67−1.80 (m)	30.9 CH_2	1.63−1.76 (m)	30.9 CH_2
13		48.4 C		44.5 C		44.5 C
14		42.3 C		47.7 C		47.8 C
15	2.22 (m)	51.2 CH_2	1.95 (m)	43.1 CH_2	1.93 (m)	43.0 CH_2
	2.03 (m)		1.60 (m)		1.65 (m)	
16		209.8 C	4.52 (dt, 5.6, 7.3)	73.1 CH	4.50 (dt, 5.5, 7.7)	73.0 CH
17		142.3 C	1.53 (m)	55.1 CH	1.52 (m)	55.1 CH
18	1.33 (s)	23.8 CH_3	0.87 (s)	16.6 CH_3	0.86 (s)	16.5 CH_3
19	0.85 (d, 4.4)	29.8 CH_2	1.11 (s)	18.6 CH_3	1.11 (s)	18.6 CH_3
	0.62 (d, 4.4)					
20		151.2 C	1.91 (m)	26.8 CH	1.83 (m)	31.3 CH
21	1.88 (s)	20.2 CH_3	0.93 (d, 6.4)	18.1 CH_3	0.94 (d, 6.4)	18.6 CH_3
22	3.27 (m)	31.4 CH_2	1.57 (m)	26.1 CH_2	1.62 (m)	32.3 CH_2
	2.21 (m)		1.35 (m)		1.07 (m)	
23	1.45−1.72 (m)	30.0 CH_2	1.66−1.84 (m)	31.3 CH_2	1.74 (m)	32.1 CH_2
					1.45 (m)	
24	3.16 (brd, 10.0)	76.2 CH	3.57 (dd, 2.4, 11.8)	75.1 CH	4.05 (dd, 4.6, 8.6)	77.2 CH
25		72.3 C		73.1 C		147.9 C
26	1.13 (s)	23.4 CH_3	1.20 (s)	26.8 CH_3	4.94 (brs)	110.8 CH_2
					4.81 (brs)	
27	1.14 (s)	26.1 CH_3	1.14 (s)	22.9 CH_3	1.72 (s)	17.8 CH_3
28	1.09 (s)	20.7 CH_3	1.07 (s)	26.2 CH_3	1.07 (s)	26.1 CH_3
29	1.04 (s)	22.1 CH_3	1.05 (s)	21.3 CH_3	1.05 (s)	21.3 CH_3
30	0.98 (d, 0.8)	21.0 CH_3	0.85 (s)	25.1 CH_3	0.84 (s)	25.2 CH_3

powder; $[\alpha]_D^{25}$ − 94.7 (*c* 0.40, MeOH); UV (MeOH) λ_{max} (log ε) 257 (3.95) nm; ECD (MeOH) $[\theta]$ −16953 (259 nm), −6852 (345 nm); ^{1}H and ^{13}C NMR data; see Table 3; positive HRESIMS *m*/*z* 493.3297 $[M + Na]^+$ (calcd for $C_{30}H_{46}O_4Na$, 493.3289).

*Isoargentatin C [(16β,20R,24R)-16,24,25-Trihydroxylanost-8-en-3-one] (**9**).* Amorphous colorless powder; $[\alpha]_D^{25}$ + 63.4 (*c* 0.20, MeOH); UV (MeOH) λ_{max} (log ε) 250 (sh, 3.07) nm; ECD (MeOH) $[\theta]$ −842 (316 nm); ^{1}H and ^{13}C NMR data; see Table 3; positive HRESIMS *m*/*z* 497.3623 $[M + Na]^+$ (calcd for $C_{30}H_{50}O_4Na$, 497.3602).

*Isoargentatin H [(16β,20R,24R)-16,24-Dihydroxylanosta-8,25-dien-3-one] (**10**).* Amorphous colorless powder; $[\alpha]_D^{25}$ + 60 (*c* 0.1, $CHCl_3$); UV (MeOH) λ_{max} (log ε) 200 (2.67) nm; ECD (MeOH) $[\theta]$ +336 (291 nm); ^{1}H and ^{13}C NMR data; see Table 3; positive HRESIMS *m*/*z* 439.3559 $[MH - H_2O]^+$ (calcd for $C_{30}H_{47}O_2$, 439.3571).

*3-Epi-quisquagenin [(3α,16β,20S,24R)-20,24-Epoxy-cycloartan-3,16,25-triol] (**11**).* Amorphous colorless powder; $[\alpha]_D^{25}$ + 34.6 (*c* 0.1, MeOH); UV (MeOH) λ_{max}(log ε) 202 (sh, 2.90) nm; ECD (MeOH) $[\theta]$ −321 (202 nm); ^{1}H and ^{13}C NMR data; see Table 4; positive HRESIMS *m*/*z* 475.3781 $[MH]^+$ (calcd for $C_{30}H_{51}O_4$, 475.3787).

*Isoquisquagenin [(3β,16β,20S,24R)-20,24-epoxy-lanost-8-en-3,16,25-triol] (**12**).* Amorphous colorless powder; $[\alpha]_D^{25}$ + 21.3 (*c* 0.2, MeOH); UV (MeOH) λ_{max} (log ε) 264 (sh, 2.39) nm, λ_{max} (log ε) 205 (sh, 2.60) nm; ECD (MeOH) $[\theta]$ +1181 (205 nm); ^{1}H and ^{13}C NMR data; see Table 4; positive HRESIMS *m*/*z* 475.3773 $[MH]^+$ (calcd for $C_{30}H_{51}O_4$, 475.3787).

*Argentatin H [(16β,20R,24R)-16,24-Dihydroxycycloart-25-en-3-one] (**13**).* Colorless amorphous solid; $[\alpha]_D^{25}$ + 31.2 (*c* 0.88, MeOH); UV (MeOH) λ_{max} (log ε) 275 (sh, 3.89) nm; ECD (MeOH) $[\theta]$ −1697 (296 nm); ^{1}H and ^{13}C NMR data;

https://doi.org/10.1021/acsomega.1c01714
ACS Omega 2021, 6, 15486−15498

Table 4. ^{1}H and ^{13}C NMR Data of 11−13 in $CDCl_3$

	11		12		13	
position	δ_H	δ_C	δ_H	δ_C	δ_H	δ_C
1	2.24 (m)	37.6 CH_2	1.71 (m)	35.1 CH_2	1.81 (m)	33.4 CH_2
	1.66 (m)		1.22 (m)		1.52 (m)	
2	1.91 (m)	28.5 CH_2	1.64 (m)	28.1 CH_2	2.68 (m)	37.5 CH_2
	1.62 (m)				2.27 (m)	
3	3.45 (m)	76.9 CH	3.21 (m)	78.9 CH		216.6 C
4		39.5 C		38.5 C		50.2 C
5	1.80 (m)	41.2 CH	1.03 (m)	50.4 CH	1.67 (m)	48.4 CH
6	1.48 (m)	21.2 CH_2	1.67 (m)	18.2 CH_2	1.53 (m)	21.4 CH_2
	0.75 (m)				0.93 (m)	
7	1.85 (m)	27.3 CH_2	2.05 (m)	20.7 CH_2	2.03 (m)	26.4 CH_2
	0.98 (m)				1.14 (m)	
8	1.64 (m)	48.0 CH		134.5 C	1.65 (m)	47.9 CH
9		19.4 C		133.7 C		20.9 C
10		25.8 C		37.0 C		26.0 C
11	1.32 (m)	25.7 CH_2	2.08 (m)	26.4 CH_2	1.36 (m)	25.9 CH_2
	1.06 (m)				1.10 (m)	
12	1.76 (m)	33.2 CH_2	1.75 (m)	31.6 CH_2	1.56−1.68 (m)	32.5 CH_2
	1.65 (m)					
13		46.2 C		47.6 C		45.3 C
14		46.7 C		45.2 C		46.7 C
15	1.98 (m)	48.5 CH_2	1.90 (m)	43.4 CH_2	1.99 (m)	47.6 CH_2
	1.47 (m)		1.78 (m)		1.35 (m)	
16	4.57 (q)	73.6 CH	4.61 (q)	74.0 CH	4.44 (dt, 4.8, 8.0)	72.6 CH
17	2.11 (d, 7.7)	55.5 CH	2.02 (d, 7.7)	54.8 CH	1.59 (m)	56.8 CH
18	1.26 (s)	25.3 CH_3	1.05 (s)	18.7 CH_3	1.15 (m)	19.0 CH_3
19	0.54 (d, 4.0)	30.4 CH_2	0.97 (s)	18.9 CH_3	0.79 (d, 4.0)	29.9 CH_2
	0.34 (d, 4.0)				0.56 (d, 4.0)	
20		87.3 C		87.1 C	1.82 (m)	31.0 CH
21	1.40 (s)	20.9 CH_3	1.30 (s)	25.8 CH_3	0.92 (d, 6.4)	18.3 CH_3
22	2.01 (m)	26.6 CH_2	2.17 (m)	37.8 CH_2	1.71 (m)	32.1 CH_2
	1.15 (m)		1.68 (m)		1.43 (m)	
23	1.92 (m)	23.8 CH_2	1.91 (m)	24.2 CH_2	1.72 (m)	33.0 CH_2
					1.40 (m)	
24	3.83 (t, 7.5)	84.5 CH	3.81 (t, 7.7)	84.3 CH	4.02 (dd, 3.2, 9.2)	77.2 CH
25		70.9 C		70.9 C		148.0 C
26	1.11 (s)	26.0 CH_3	1.11 (s)	26.0 CH_3	4.92 (brs)	110.7 CH_2
					4.79 (brs)	
27	1.22 (s)	27.4 CH_3	1.22 (s)	27.8 CH_3	1.71 (s)	17.8 CH_3
28	0.86 (s)	20.3 CH_3	0.83 (s)	25.2 CH_3	1.07 (s)	20.8 CH_3
29	0.86 (s)	21.1 CH_3	0.80 (s)	15.4 CH_3	1.02 (s)	22.1 CH_3
30	0.93 (s)	26.1 CH_3	0.98 (s)	27.9 CH_3	0.86 (s)	20.8 CH_3

see Table 4; positive HRESIMS m/z 479.3494 $[M + Na]^+$ (calcd for $C_{30}H_{48}O_3Na$, 479.3496).

Preparation of (*R*)- and (*S*)-MTPA Esters of 4, 7, and 10. Each triterpenoid (**4**, **7**, or **10**; 1.0 mg) was dissolved in pyridine-d_5 (0.5 mL), and the solution was transferred into a dry NMR tube. (*S*)-(−)-α-Methoxy-α-(trifluoromethyl)-phenylacetyl chloride [(*S*)-MTPA chloride] (5.0 μL) was added to the NMR tube immediately under a stream of N_2 and was shaken carefully to mix the sample and MTPA chloride. The NMR tube was allowed to stand at 25 °C for 1 h to afford the (*R*)-MTPA ester derivatives (**4a**, **7a**, and **10a**). Another portion of **4**, **7**, or **10** (1.0 mg) in pyridine-d_5 was reacted in a second NMR tube with (*R*)-(+)-α-methoxy-α-(trifluoromethyl)-phenylacetyl chloride [(*R*)-MTPA chloride] (5.0 μL) at 25 °C for 1 h to afford the (*S*)-MTPA ester derivatives (**4b**, **7b**, and **10b**). ^{1}H NMR data of **4a** (400 MHz, pyridine-d_5): δ 5.718 (m, 1H, H-24), 5.191 (brs, 1H, H-26a), 5.011 (brs, 1H, H-26b), 2.234 (m, 1H, H-20), 2.102 (m, 1H, H-23a), 1.811 (m, 1H, H-23b), 1.800 (s, 3H, H_3-27), 1.754 (m, 1H, H-22b), 1.136 (m, 1H, H-22a), 1.001 (d, J = 6.2 Hz, 3H, H_3-21); ^{1}H NMR data of **4b** (400 MHz, pyridine-d_5): δ 5.678 (m, 1H, H-24), 5.076 (brs, 1H, H-26a), 4.952 (brs, 1H, H-26b), 2.286 (m, 1H, H-20), 2.124 (m, 1H, H-23a), 1.884 (m, 1H, H-23b), 1.763 (m, 1H, H-22a), 1.660 (s, 3H, H_3-27), 1.402 (m, 1H, H-22b), 1.049 (d, J = 6.2 Hz, 3H, H_3-21).; ^{1}H NMR data of **7a** (400 MHz, pyridine-d_5): δ 5.620 (m, 1H, H-24), 2.312 (d, J = 7.8 Hz, 1H, H-17), 1.920 (m, 2H, H_2-23), 1.800 (m, 1H, H-20), 1.500 (s, 6H, H_3-26, H_3-27), 1.400 (m, 2H, H_2-22), 0.930 (d, J = 5.6 Hz, 3H, H_3-21); ^{1}H NMR data of **7b** (400 MHz, pyridine-d_5): δ 5.630 (m, 1H, H-24), 2.420 (d, J = 7.9 Hz, 1H, H-17), 2.050 (m, 2H, H_2-23), 1.970 (m, 1H, H-20), 1.700 (m, 2H, H_2-22), 1.440 (s, 3H, H_3-26), 1.430 (s, 3H, H_3-27), 1.080 (d, J = 6.7 Hz, 3H, H_3-21); ^{1}H NMR data of **10a** (400 MHz, pyridine-d_5): δ 5.699 (m, 1H, H-24), 5.140 (brs, 1H, H-26a),

https://doi.org/10.1021/acsomega.1c01714
ACS Omega 2021, 6, 15486−15498

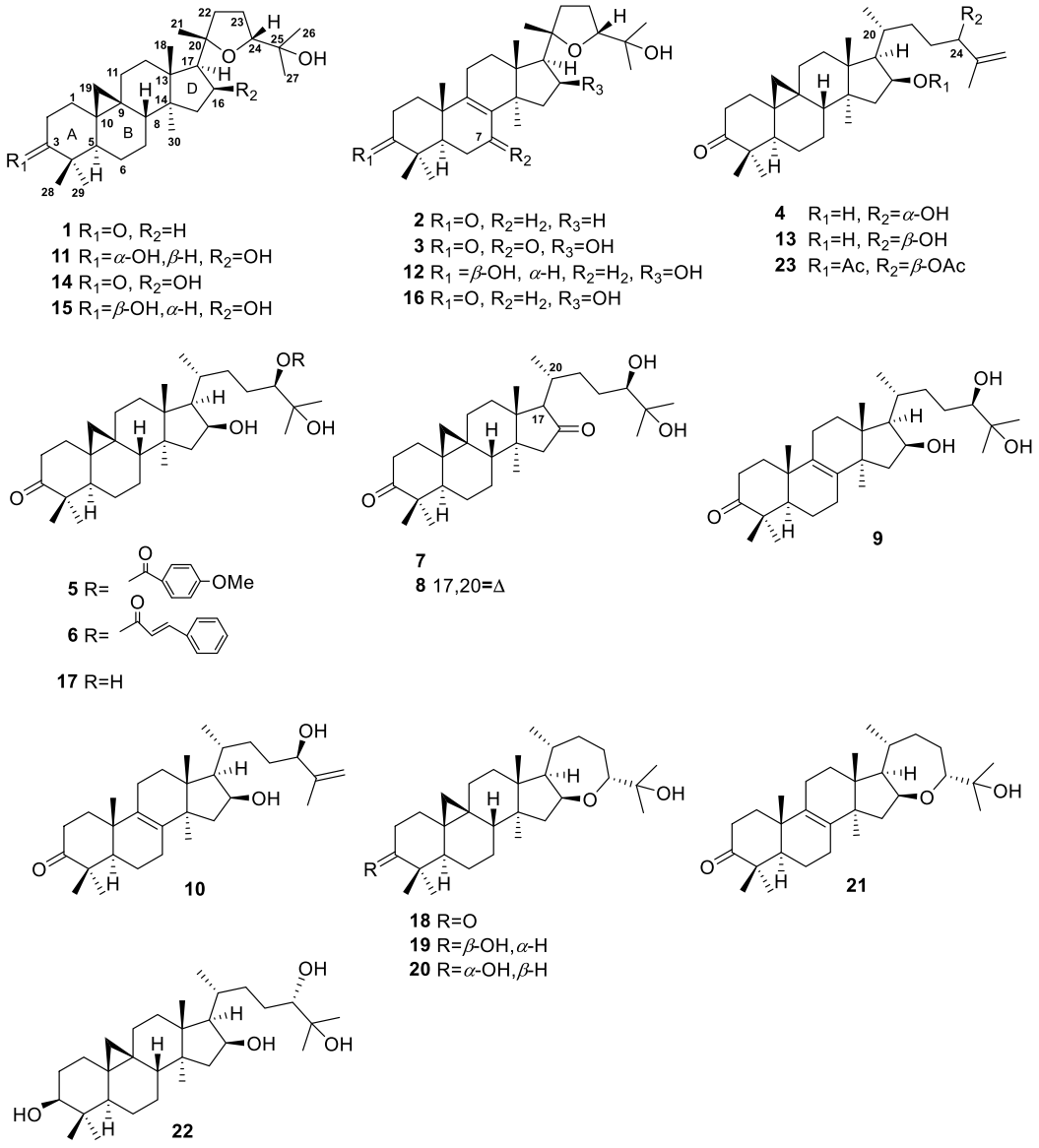

Figure 1. Structures of triterpenoids **1**−**22** from guayule resin and diacetylargentatin H (**23**).

5.010 (brs, 1H, H-26b), 2.680 (m, 1H, H-20), 2.022 (m, 2H, H_2-23), 1.782 (m, 2H, H_2-22), 1.669 (s, 3H, H_3-27), 1.069 (d, J = 6.2 Hz, 3H, H_3-21); ^{1}H NMR data of **10b** (400 MHz, pyridine-d_5): δ 5.751 (m, 1H, H-24), 5.232 (brs, 1H, H-26a), 5.051 (brs, 1H, H-26b), 2.258 (m, 1H, H-20), 1.999 (m, 2H, H_2-23), 1.802 (s, 3H, H_3-27), 1.776 (m, 2H, H_2-22), 1.062 (d, J = 6.2 Hz, 3H, H_3-21).

Hydrolysis of 5 and 6. A solution of the triterpene ester **5** or **6** (0.1 mg) in MeOH (0.1 mL) containing Na_2CO_3 (0.1 mg) was stirred at 25 °C for 2 h (TLC control). TLC [silica gel, $CHCl_3$/MeOH (95:5)] and HPLC [RP C_{18}, MeOH/H_2O (85:15), t_R = 24.1 min)] comparison of the resulting product with an authentic sample confirmed the hydrolysis product to be identical to argentatin C (**17**).

Acetylation of Argentatin H (13). To a solution of **13** (2.2 mg) in anhydrous pyridine (0.5 mL) was added Ac_2O (0.5 mL), and the mixture was stirred at 25 °C for 6 h (TLC control), after which it was poured into ice/water (10.0 mL) and extracted with EtOAc (3 × 10.0 mL). The EtOAc extracts were combined and washed with H_2O (3 × 5.0 mL), dried over anhydrous Na_2SO_4, and evaporated under reduced pressure. The crude product thus obtained was separated by silica gel (1.0 g) column chromatography. Elution with $CHCl_3$/MeOH (99:1, v/v) afforded the acetylated product (2.3 mg), which was identified as argentatin H diacetate (**23**) by comparison of its ^{1}H and ^{13}C NMR data with those reported.[8]

Reduction of Argentatin A (14) to 3-*Epi*-quisquagenin (11) and Quisquagenin (15). To a stirred solution of **14** (25.0 mg) in MeOH (10.0 mL) at 0 °C was added $NaBH_4$ (3.0 mg), and stirring was continued at this temperature until the disappearance of the starting material (TLC control). The reaction was then quenched with ice-cold water (10.0 mL), concentrated under reduced pressure, and extracted with EtOAc (3 × 10.0 mL). The EtOAc extracts were combined and washed with H_2O (3 × 5.0 mL), dried over anhydrous Na_2SO_4, and evaporated under reduced pressure. The crude product (25.0 mg) thus obtained was separated by RP-HPLC (MeOH−H_2O; 82.5:17.5) to afford major [21.5 mg, 85%; t_R 30.5 min; $[\alpha]_D^{25}$ + 47.4 (c 0.2, MeOH)] and minor [1.5 mg, 6%; t_R 34.5 min; $[\alpha]_D^{25}$ + 34.2 (c 0.1, MeOH)] products as white solids. These were identified as quisquagenin (**15**) and

https://doi.org/10.1021/acsomega.1c01714
ACS Omega 2021, 6, 15486−15498

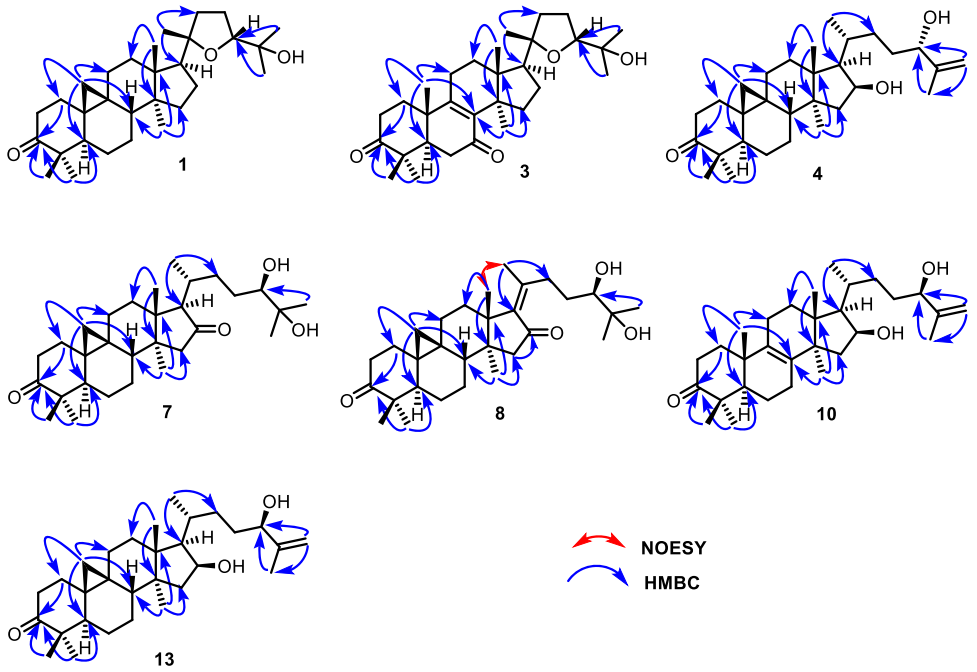

Figure 2. Key HMBC correlations of **1**, **3**, **4**, **7**, **8**, **10**, and **13** and key NOESY correlation of **8**.

3-*epi*-quisquagenin (**11**), respectively, by comparison of their ^{1}H and ^{13}C NMR data with those of the natural products obtained above.

Reduction of Isoargentatin A (16) to Isoquisquagenin (12). To a stirred solution of isoargentatin A (**16**, 4.0 mg) in MeOH (2.0 ml) at 0 °C was added $NaBH_4$ (1.0 mg), and the reaction mixture was stirred at 0 °C until the disappearance of the starting material (TLC control). The reaction mixture was quenched with ice-cold water (5.0 mL), concentrated under reduced pressure, and extracted with EtOAc (3 × 5.0 mL). The EtOAc extracts were combined and washed with H_2O (3 × 2.0 mL), dried over anhydrous Na_2SO_4, and evaporated under reduced pressure to afford isoquisquagenin (**12**) (4.0 mg, 99%) as a white solid; $[\alpha]_D^{25}$ + 21.6 (*c* 0.15, MeOH); ^{1}H and ^{13}C NMR data were identical to those of the natural product obtained above.

Cytotoxicity Assay. The tetrazolium-based colorimetric (MTT) assay was employed for evaluation of cytotoxic activity of samples against the sentinel cancer cell lines, human non-small cell lung (NCI-H460), human CNS glioma (SF-268), and human breast (MCF-7). Compounds were also tested versus human prostate adenocarcinoma (PC-3M), human metastatic breast adenocarcinoma (MDA-MB-231), and normal human lung fibroblast (WI-38) cells as described previously.[17] Doxorubicin and dimethyl sulfoxide (DMSO) were used as positive and negative controls, respectively.

RESULTS AND DISCUSSION

Characterization of Compounds. The resin of the *P. argentatum* line AZ-2 obtained as a byproduct from Bridgestone Americas, Inc. rubber production was fractionated by solvent−solvent partitioning, size permeation chromatography, and silica gel chromatography. The resulting fractions were further purified by preparative TLC and/or HPLC to afford 19 triterpenoids. Nine of these were identified as argentatin A (**14**),[5a] quisquagenin (**15**),[18] *iso*-argentatin A (**16**),[7a] argentatin C (**17**),[5a] argentatin B (**18**),[5a] argentatin D (**19**),[5a,19] 3-*epi*-argentatin D (**20**),[5a,19] *iso*-argentatin B (**21**),[7a] and cyclofoetigenin A (**22**)[20] by comparison of their ^{1}H and ^{13}C NMR spectroscopic data with those reported for these compounds. It should be noted that 3-*epi*-argentatin D (**20**) has been incorrectly referred as isoargentatin D.[21] In order to avoid similar confusions, here, we provide systematic names for all new compounds based on their triterpenoid skeletons (Figure 1).

Triterpenoid **1** was determined to have the molecular formula $C_{30}H_{48}O_3$ from its HRESIMS and NMR data and indicated 7 degrees of unsaturation. The ^{1}H NMR spectrum of **1** (Table 1) exhibited seven singlet methyls [δ_H 0.91 (H_3-30), 1.03 (H_3-28), 1.08 (H_3-29), 1.13 (H_3-27), 1.14 (H_3-18), 1.21 (H_3-26), and 1.22 (H_3-21)], an oxygenated methine [δ_H 3.75 (d, J = 7.0, 8.2 Hz, H-24)], and a pair of doublets [δ_H 0.56 (d, J = 4.0 Hz, H-19) and 0.76 (d, J = 4.0 Hz, H-19)], typical of geminal methylene protons of a tetra-substituted cyclopropane ring, characteristic of a cycloartane-type triterpenoid.[22] The ^{13}C NMR spectrum of **1** (Table 1) assigned with the help of HSQC and HMBC data (Figure 2 and Figures S4 and S5 in the Supporting Information) and comparison of these data with those of argentatin A (**14**)[7a] indicated that the only difference between **1** and **14** is that the oxygenated methine (CHOH-16) signal of **14** was replaced by a methylene signal [δ_C 25.1 (CH_2-16)] in **1**. The signal due to CH_2-15 in the ^{13}C NMR spectrum of **1** displayed a high-field shift compared to that of **14** due to the absence of the β-effect of substituent perturbations by the OH group at C-16.[23] Thus, the structure of **1** was determined as 16-deoxyargentatin A [(20*S*,24*R*)-20,24-epoxy-25-hydroxycycloartan-3-one].

The HRESIMS and ^{1}H and ^{13}C NMR spectroscopic data of triterpenoid **2** were consistent with the molecular formula $C_{30}H_{48}O_3$, indicating 7 degrees of unsaturation. In its ^{1}H NMR spectrum, **2** exhibited eight singlet methyl signals characteristic of lanostane-type triterpenoids[7a] bearing a 19-methyl, 8(9)-ene and a side-chain tetrahydrofuran moiety. Comparison of the ^{1}H NMR data of **2** (Table 1) with those of isoargentatin A

https://doi.org/10.1021/acsomega.1c01714
ACS Omega 2021, 6, 15486−15498

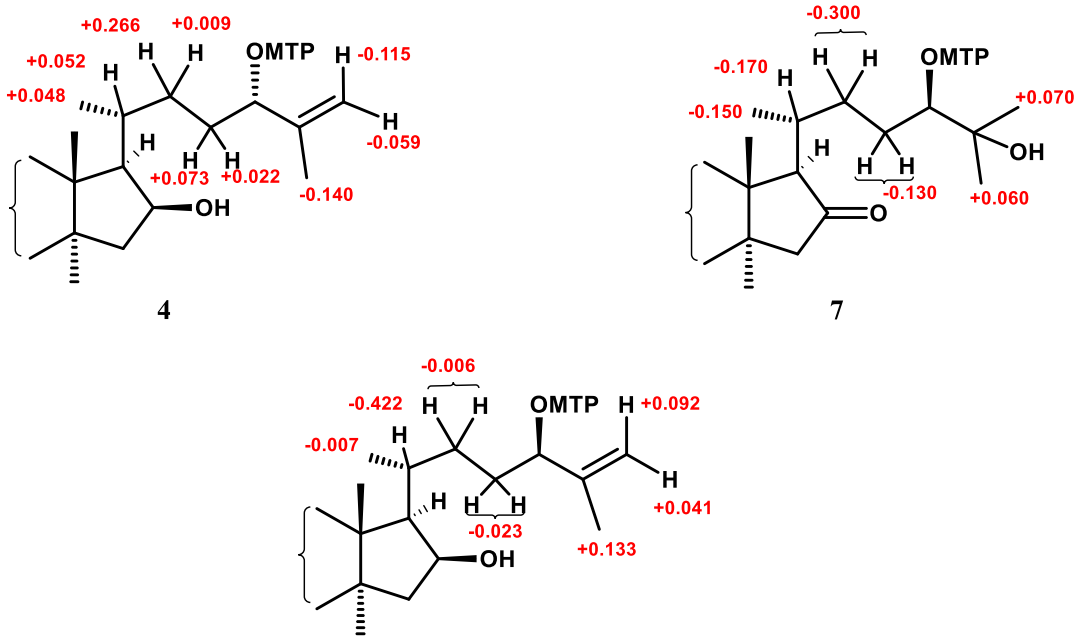

Figure 3. $\Delta\delta$ values [$\Delta\delta$ values (in ppm) = $\delta_S - \delta_R$] obtained for (*S*)- and (*R*)-MTPA esters of **4**, **7**, and **10**.

(**16**) which was found to co-occur in this resin sample indicated that unlike **16**, which has two oxygenated methine protons, **2** contained only one of these protons [δ_H 3.74 (dd, *J* = 7.1, 7.9 Hz)] suggesting that **2** is probably the 16-deoxygenated analogue of **16**. Analysis of the ^{13}C NMR spectrum of **2** with the help of HSQC and HMBC data and comparison of the ^{13}C NMR data with those of isoargentatin A (**16**)[7a] confirmed that the major structural differences between **2** and **16** are due to the substituents in ring D. These data also suggested that the oxygenated methine moiety (CHOH-16) of **16** was replaced by a methylene moiety [δ_C 25.1, CH_2-16] in **2**. On the basis of the foregoing evidence, the structure of **2** was determined as 16-deoxyisoargentatin A [(20*S*,24*R*)-20,24-epoxy-25-hydroxylanost-8-en-3-one].

The molecular formula of triterpenoid **3** was determined as $C_{30}H_{46}O_5$ on the basis of its HRESIMS and NMR data, indicating 8 degrees of unsaturation. The ^{1}H NMR spectrum of **3** (Table 1) exhibited signals due to two oxygenated methines [δ_H 3.82 (dd, *J* = 8.0 Hz, H-24), 4.68 (dd, *J* = 8.0), 13.6 Hz, H-16] similar to isoargentatin A (**16**) in addition to eight singlet methyl signals characteristic of lanostane-type triterpenoids bearing a 19-methyl, 8(9)-ene, and a side-chain tetrahydrofuran ring.[7a] However, its ^{13}C NMR spectrum (Table 1) indicated the presence of signals due to two carbonyl carbons [δ_C 218.2 (C-3), 198.4 (C-7)] compared to **16**, which contains only the C-3 carbonyl group. The second carbonyl of **3** was located at C-7 by the HMBC correlations of H_3-19 [δ_H 1.08 (s)]/C-9 (δ_C 164.0) and H_3-30 [δ_H 1.10 (s)]/C-8 (δ_C 138.3). Based on the above evidence, the structure of **3** was determined as 7-oxoisoargentatin A [(16β,20*S*,24*R*)-20,24-epoxy-16,25-dihydroxylanost-8-en-3,7-dione].

Triterpenoid **4** was determined to have the molecular formula $C_{30}H_{48}O_3$ by the analysis of its HRESIMS and NMR data, indicating 7 degrees of unsaturation. The ^{1}H NMR spectrum (Table 2) of **4** showed six methyl signals, two oxygenated methines, a pair of olefinic methylene signals, and a pair of doublets due to geminal protons of a tetra-substituted cyclopropane moiety typical of cycloartane-type triterpenoids. The ^{13}C NMR spectrum of **4** (Table 2) exhibited 30 signals including those due to carbonyl [δ_C 216.5 (C-3)], olefinic [δ_C 147.9 (C-25) and 110.2 (C-26)], and oxygenated [δ_C 72.8 (CH-16) and 72.9 (CH-24)] carbons. These data indicated that **4** has the same carbon skeleton as argentatin C (**17**),[7b] and HMBC correlation analysis of **4** (Figure 2) confirmed that its planar structure is the same as that of argentatin H (**13**),[8] both of which are cometabolites of guayule resin (see below). The β-orientation of 16-OH in **4** was supported by the NMR chemical shifts of C-16 and H-16 and the ^{1}H NMR coupling pattern of H-16, which is similar to that of **13**. The forgoing suggested **4** differed from argentatin H (**13**) only due to the configuration of the OH group at C-24. The absolute configuration of the chiral center at C-24 of **4** was determined to be *S* by the application of the modified Mosher's ester method (Figure 3).[24] Therefore, the structure of **4** was determined as 24-*epi*-argentatin H [(16β,20*R*,24*S*)-16,24-dihydroxycycloart-25-en-3-one].

The HRESIMS and ^{1}H and ^{13}C NMR spectroscopic data of **5** were consistent with the molecular formula $C_{38}H_{56}O_6$, suggesting 11 degrees of unsaturation and indicating that it contained eight carbons more than that of a typical cycloartane or lanostane triterpenoid. The ^{1}H NMR spectrum of **5** (Table 2) exhibited the signals characteristic of a *p*-anisoyl group [δ_H 6.91 (2H, d, *J* = 8.8 Hz, H-3′/5′), 7.99 (2H, d, *J* = 8.8 Hz, H-2′/6′), 3.85 (3H, s, 4′-OMe)] besides those of a cycloartane-type triterpenoid including seven methyls, two oxygenated methines, and a pair of signals of a tetra-substituted cyclopropane moiety. The ^{13}C NMR spectrum of **5** (Table 2) analyzed with the help of HSQC and HMBC data exhibited thirty signals resembling those of argentatin C (**17**)[7a] and six additional signals [δ_C 166.5 (C-8′), 164,5 (C-7′), 131.7 (CH-2′/6′), 122.4 (C-1′), 113.7 (CH-3′/5′), and 55.5 (CH_3-8′)], confirming the presence of a *p*-anisoyl substituent in **5**. Careful comparison of the ^{13}C NMR data of **5** with those of argentatin C (**17**)[7b] suggested that the chemical shift of C-24 of **5** had moved to downfield (2.5−3.0 ppm) compared to that of **17**, indicating that the *p*-anisoyl group is attached to the OH group

https://doi.org/10.1021/acsomega.1c01714
ACS Omega 2021, 6, 15486−15498

at C-24.[25] The configuration at C-24 of **5** was deduced to be *R*, same as that of **17** by comparison of their ^{13}C NMR chemical shift data. This was confirmed by the hydrolysis ($NaCO_3$/MeOH) of **5**, affording a product identical (^1H and ^{13}C NMR) to argentatin C (**17**). Based on foregoing information, compound **5** was identified as 24-*O*-*p*-anisoylargentatin C [(16*β*,20*R*,24*R*)-24-*p*-anisoyloxy-16,25-dihydroxycycloartan-3-one].

Compound **6** was determined to have the molecular formula $C_{39}H_{56}O_5$ by the analysis of its HRESIMS and NMR data, indicating 12 degrees of unsaturation. The ^1H and ^{13}C NMR spectroscopic data of **6** (Table 2) were almost identical to those of **5** except for the signals due to the substituent acyl group, suggesting that **6** is also a 24-*O*-acylated analogue of argentatin C (**17**). This acyl substituent of **6** was determined to be a *trans*-cinnamoyl group by its characteristic ^1H NMR [δ_H 6.47 (1H, d, J = 15.6 Hz, H-8′), 7.71 (1H, d, J = 15.6 Hz, H-7′), 7.52 (2H, m, H-2′/6′), 7.38 (3H, m, H-3′/5′ and H-4′)] and ^{13}C NMR [δ_C 167.3 (C-9′), 145.6 (CH-7′), 134.3 (CH-4′ and C-1′), 128.9 (CH-3′/5′), 128.2 (CH-2′/6′), and 117.8 (CH-8′)] data. Hydrolysis ($NaCO_3$/MeOH) of **6** afforded argentatin C (**17**), confirming the identity of **6** as 24-*O*-*trans*-cinnamoylargentatin C [(16*β*,20*R*,24*R*)-24-*trans*-cinnamoyloxy-16,25-dihydroxycycloartan-3-one].

Triterpenoid **7** exhibited a $[MH - H_2O]^+$ ion at m/z 455.3509 in its HRESIMS, consistent with the molecular formula $C_{30}H_{48}O_4$, indicating 7 degrees of unsaturation. The ^1H NMR data of **7** suggested it to be an analogue of argentatin C (**17**) as it contained signals due to seven methyls in addition to the tetra-substituted cyclopropane moiety (Table 2). Complete analysis of the ^{13}C NMR spectrum of **7** with the help of HMBC data (Figure 2) suggested that it contained signals due to two ketone carbonyls [δ 216.0 (C-3) and 221.3 (C-16)] besides those typical of the triterpenoid skeleton. Comparison of these data with those of argentatin C (**17**) located the additional carbonyl group at C-16, indicating that the CHOH moiety of **17** at this position has undergone oxidation to a C=O moiety. The signal due to C-24 of **7** appeared at 75.9 ppm in its ^{13}C NMR spectrum similar to that of **17**, indicating that **7** has the same *R* configuration at C-24 as argentatin C (**17**). This was confirmed by the application of the modified Mosher's ester method (Figure 3).[24] Thus, the structure of **7** was determined as 16-dehydroargentatin C [(20*R*,24*R*)-24,25-dihydroxycycloartan-3,16-dione].

The HRESIMS and ^{13}C NMR spectroscopic data of **8** were consistent with the molecular formula $C_{30}H_{46}O_4$ and indicated 8 degrees of unsaturation. The ^1H NMR spectrum of **8** (Table 4) exhibited signals due to seven methyl groups and a pair of signals characteristic of geminal methylene protons of a tetra-substituted cyclopropane ring, suggesting that **8** is an argentatin C-type triterpenoid. These ^1H NMR data also indicated that the signal due to H_3-21 that usually appears at δ_H 0.92−0.95 as a doublet (J = 6.2−6.6 Hz) in these triterpenoids has moved downfield to δ_H 1.88 and appeared as a singlet in **8**, suggesting that this methyl group is attached to a sp^2 carbon of a double bond. The ^{13}C NMR spectrum of **8** analyzed with the help of HMBC data (Figure 2) showed the presence of signals due to two ketone carbonyls (δ_C 221.3 and 209.8) and a double bond (δ_C 142.3 and 151.2) besides those typical of the triterpenoid skeleton. The additional degree of unsaturation in **8** compared to 16-dehydroargentatin C (**7**) was attributable to this double bond and the low-field shift of the C-16 carbonyl carbon from δ_C 221.3 to 209.8 ppm in its ^{13}C NMR spectrum indicated that this double bond is in conjugation with C-16 carbonyl moiety. Analysis of the HMBC data confirmed the presence of a 17(20)-en-16-one moiety in **8** (Figure 2). The ^{13}C NMR signal due to C-24 of **8** appeared at δ_C 76.2 ppm, almost the same as that of argentatin C (**17**), suggesting that **8** has the same *R* configuration at C-24 as in **17**. The configuration of the C-17(20) double bond was assigned as *Z* by the NOESY correlation between H_3-18 (δ_H 1.33) and H_3-21 (δ_H 1.88) (Figure 2). Based on the foregoing evidence, the structure of **8** was determined as 16,17(20)-didehydroargentatin C [(20*R*,24*R*)-24,25-dihydroxycycloart-17(20)-en-3,16-dione].

The molecular formula of triterpenoid **9** was determined as $C_{30}H_{50}O_4$ by its HRESIMS and ^{13}C NMR spectroscopic data and indicated 6 degrees of unsaturation. The ^1H NMR spectrum of **9** (Table 3) exhibited signals due to eight methyl groups. These data and the absence of typical signals due to the cyclopropane moiety in its ^1H NMR spectrum suggested that **9** is a lanostane-type triterpenoid.[7b] The ^{13}C NMR spectrum of **9** showed 30 signals including those due to eight methyls, a ketone carbonyl, two olefinic carbons, and three oxygenated carbons (Table 3). The NMR signals due to the side-chain moiety were almost identical to those of argentatin C (**17**).[7b] These data suggested that in **9**, the cyclopropane moiety of **17** is replaced with CH_3-19 and 8,9-ene moieties, resulting in a lanostane-type triterpenoid. Therefore, the structure of **9** was determined as isoargentatin C [(16*β*,20*R*,24*R*)-16,24,25-trihydroxylanost-8-en-3-one].

Triterpenoid **10** was determined to have the molecular formula $C_{30}H_{48}O_3$ by the analysis of its HRESIMS and NMR data, indicating 7 degrees of unsaturation. The ^1H and ^{13}C NMR spectroscopic data of **10** (Table 3) analyzed with the help of HMBC data (Figure 2) resembled closely to those of isoargentatin C (**9**) but contained a side chain with a gem-disubstituted olefin moiety [δ_H 4.81 (brs, 1H) and 4.94 (brs, 1H); δ_C 110.8 and 147.9] bearing a methyl group [δ_H 1.71 (s, 3H); δ_C 17.8] instead of the terminal *iso*-propanol group in **9**. These data and comparison of their molecular formulae suggested that **10** may be the 25,26-ene analogue resulting from isoargentatin C (**9**) by the loss of a molecule of water. This was supported by the HMBC correlations of H-26 (δ_H 4.94 and 4.81)/CH_3-27 (δ_C 17.8) and H-26/CH-24 (δ_C 77.2) (Figure 2). The ^{13}C NMR chemical shift of CH-24 (δ_C 77.2 ppm) was almost the same as that of argentatin H (**13**), suggesting *R* configuration for C-24. This was further confirmed by the application of the modified Mosher's ester method (Figure 3).[24] Triterpenoid **10** was thus identified as isoargentatin H [(16*β*,20*R*,24*R*)-16,24-dihydroxylanosta-8,25-dien-3-one].

The HRESIMS and ^{13}C NMR spectroscopic data of triterpenoids **11** and **12** were consistent with the molecular formula $C_{30}H_{50}O_4$ and indicated 6 degrees of unsaturation. The ^1H and ^{13}C NMR spectra of **11** (Table 4) exhibited signals due to seven methyls, three oxygenated methines, and a tetra-substituted cyclopropane moiety, characteristic of cycloartane-type triterpenoids.[22] The presence of three oxygenated methine signals at δ_C 84.5 (C-24), 76.9 (C-3), and 73.6 (C-16) in the ^{13}C NMR spectrum of **11** suggested that it has a structure closely related to that of quisquagenin (**15**) [δ_C 84.5 (C-24), 78.7 (C-3), and 73.4 (C-16)].[18] These data suggested that **11** and **15** had close structural similarities except for the orientation of the OH group at C-3. This was confirmed by the reduction ($NaBH_4$/MeOH) of the corresponding C-3 ketone,

https://doi.org/10.1021/acsomega.1c01714
ACS Omega 2021, 6, 15486−15498

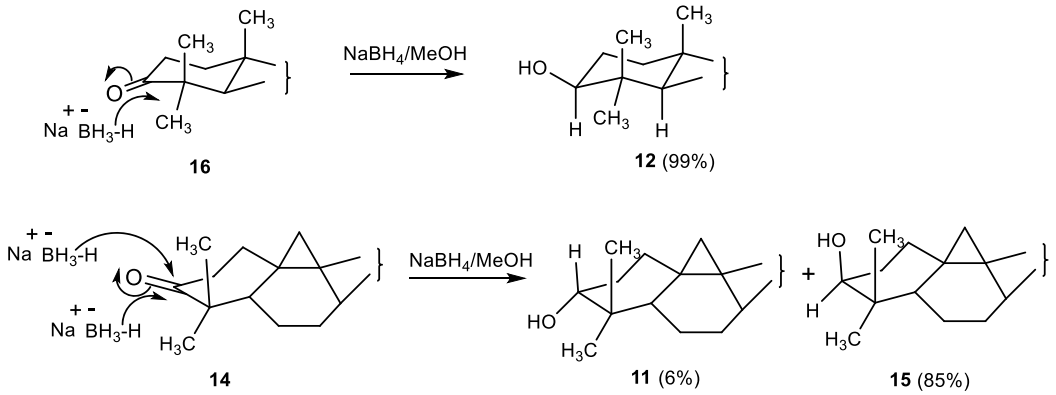

Figure 4. Chemical conversion of isoargentatin A (**16**) to isoquisquagenin (**12**) and argentatin A (**14**) to 3-*epi*-quisquagenin (**11**) and quisquagenin (**15**).

Table 5. Cytotoxicity (IC_{50}) Data for 13, 14, and 18 against Cancer Cell Lines and Normal Cells[a]

	Cell lines[b]					
Compound	PC-3M	NCI-H460	MCF-7	SF-268	MDA-MB-231	WI-38
13	21.8 ± 2.7	19.6 ± 1.3	15.2 ± 0.7	24.3 ± 0.3	22.3 ± 0.5	19.0 ± 0.7
14	31.9 ± 0.7	31.2 ± 0.0	32.8 ± 1.2	35.0 ± 0.2	32.9 ± 0.1	41.4 ± 2.8
18	13.5 ± 1.7	17.5 ± 0.9	23.1 ± 0.4	31.2 ± 1.7	32.0 ± 0.8	21.0 ± 2.9
Doxorubicin	0.25 ± 0.02	0.05 ± 0.01	0.32 ± 0.09	0.45 ± 0.07	0.67 ± 0.11	0.80 ± 0.10

[a]Results are expressed as IC_{50} values in μM. Doxorubicin and DMSO were used as positive and negative controls. [b]Key: PC-3M = metastatic human prostate adenocarcinoma; NCI-H460 = human non-small cell lung cancer; MCF-7 = human breast cancer; SF-268 = human CNS cancer (glioma), MDA-MB-231 = human metastatic breast adenocarcinoma; WI-38 = normal human lung fibroblast cells.

argentatin A (**14**), affording **15** (85% yield) and **11** (6% yield) having $[\alpha]_D$, ^{1}H, and ^{13}C NMR data identical to the natural products encountered in this work. This product distribution can be explained by taking into consideration the reducing agent ($NaBH_4$) approaching mainly from the less sterically hindered α face of the molecule (Figure 4). Thus, compound **11** was identified as 3-*epi*-quisquagenin [(3α,16β,20*S*,24*R*)-20,24-epoxy-cycloartan-3,16,25-triol].

The ^{1}H and ^{13}C NMR data of **12** (Table 4) closely resembled those of quisquagenin (**15**)[18] except for the absence of signals due to the cyclopropane moiety. Instead, **12** contained an additional methyl group [δ_H 0.97 (s, H_3-19); δ_C 18.9 (C-19)] and a tetra-substituted double bond [δ_C 134.5 (C-8) and 133.7 (C-9)], suggesting that it is a lanostane-type triterpenoid.[7a] The presence of signals due to three oxygenated methines [δ_H 4.61 (q), 3.81 (t, J = 15.2 Hz), and 3.21 (m); δ_C 84.3 (CH), 78.9 (CH), 74.0 (CH)] in its ^{1}H and ^{13}C NMR spectra and comparison of these data with those of isoargentatin A (**16**) indicated that **12** contained a CHOH moiety at C-3 instead of carbonyl moiety in **16**. This was confirmed by the reduction ($NaBH_4$/MeOH) of C-3 carbonyl group of **16**, affording **12** in 99% yield. Formation of **12** with a β-OH at C-3 as the sole product is known for related 3-keto steroids[26] and can be explained by taking into account the reducing agent ($NaBH_4$) approaching from the less sterically hindered α face of the molecule (Figure 4). Thus, compound **12** was identified as isoquisquagenin [(3β,16β,20*S*,24*R*)-20,24-epoxy-lanost-8-en-3,16,25-triol]. A literature search revealed that a compound with the gross structure as in **12** has been reported previously[27] but with unspecified stereochemistry.

Triterpenoid **13** exhibited a $[M + Na]^+$ ion at m/z 479.3494 in its HRESIMS, consistent with the molecular formula $C_{30}H_{48}O_3$, indicating 7 degrees of unsaturation. The ^{1}H and ^{13}C NMR spectra of **13** (Table 4) analyzed with the help of HSQC data were very similar to those of 24-*epi*-argentatin H (**4**) obtained above, suggesting that **13** is the 24-epimer of **4** and should be identical to argentatin H. Argentatin H has previously been characterized as its diacetate (**23**)[8] but with undefined absolute stereochemistry at C-24. Acetylation (Ac_2O/pyridine) of **13** afforded its diacetate with ^{1}H and ^{13}C NMR data identical to those reported for argentatin H diacetate (**23**).[8] Since the absolute configuration at C-24 of **4** was determined to be *S* (see above and Figure 3), argentatin H should have *R* absolute configuration at this position. Thus, argentatin H was identified as (16β,20*R*,24*R*)-16,24-dihydroxycycloart-25-en-3-one (**13**). Careful inspection of the ^{13}C NMR data for **4** and **13** suggested that the γ-effect of the chiral center C-20 can be used to distinguish the stereochemistry of C-24. The *R* isomer (**13**) has weaker γ-effect, which results in C-20 (δ_C 31.0) and C-24 (δ_C 77.2) at lower-field compared to those of the *S* isomer (**4**), which appeared at δ_C 27.2 ppm for C-20 and δ_C 72.9 ppm for C-24. These differences may be utilized in future studies to determine the stereochemistry of C-24 of triterpenoids with similar side chains.

Cytotoxic Activity. Previous reports of cytotoxic activity of cycloartane and lanostane types of triterpenoids including argentatins prompted us to evaluate **1**−**22** for their cytotoxic activity in a panel of three sentinel human cancer cell lines MCF-7 (breast adenocarcinoma), NCI-H460 (non-small cell lung), and SF-268 (CNS glioma), two metastatic cancer cell lines MDA-MB-231 (breast adenocarcinoma) and PC-3M (prostate adenocarcinoma), and normal lung epithelial cells (WI-38). Initially, a test concentration of 35 μM was selected based on recently reported *in vitro* cytotoxic activity for argentatin A (**14**).[13] Cytotoxicity assay data revealed that at this concentration most of the triterpenoids showed weak to moderate inhibition (Table S1 in the Supporting Information). Among these, argentatin H (**13**), argentatin A (**14**), and

https://doi.org/10.1021/acsomega.1c01714
ACS Omega 2021, 6, 15486−15498

argentatin B (**18**) were selected for further evaluation based on their activities and availability. Their IC_{50} (concentration required to kill 50% of cells) data (Table 5) suggested that **13** and **18** were more cytotoxic than **14** to all cancer and normal cells tested, but **14** had moderate selectivity for all cancer cell lines compared to normal cells. It was also found that the cytotoxic activity (IC_{50} = 31.9−35.0 μM) of argentatin A (**14**) for the cell lines tested for 72 h is slightly better than the activity (IC_{50} = 43.2−61.3 μM) reported for **14** for a series of colon cancer cell lines.[13] It is also noteworthy that the cytotoxic activity of argentatin B (**18**) is ca. 2-fold higher than that of argentatin A (**14**) for some cancer cell lines, suggesting the possible effect of structure on cytotoxic activity of these triterpenoids. We are currently investigating the effect of structural modification of major triterpenoid constituents of guayule resin on their biological activities, and outcomes of these studies will be reported in due course.

In conclusion, detailed investigation of the resin of *P. argentatum* AZ-2, a byproduct of guayule rubber production, led to the isolation, identification, and cytotoxicity evaluation of 12 new and 10 known cycloartane- and lanostane-type triterpenoids. The cytotoxic activity of argentatin A (**14**), together with its recently demonstrated promising antitumor activity in a mouse xenograft model of human colon cancer with no adverse toxicity,[15] warrants further investigation of cycloartane-type triterpenoids for their development as potential anticancer agents. Furthermore, the relative cytotoxic activities associated with argentatin H (**13**), argentatin A (**14**), and argentatin B (**18**) suggest the possibility of structural modification of major triterpenoids of guayule resin into value-added products with potential anticancer activity.

■ ASSOCIATED CONTENT

Supporting Information

The Supporting Information is available free of charge at https://pubs.acs.org/doi/10.1021/acsomega.1c01714.

Spectroscopic data including 1D and 2D NMR of new compounds **1**−**13** (PDF)

■ AUTHOR INFORMATION

Corresponding Author

A. A. Leslie Gunatilaka − *Southwest Center for Natural Products Research, School of Natural Resources and the Environment, College of Agriculture and Life Sciences, University of Arizona, Tucson, Arizona 85706, United States;* orcid.org/0000-0001-9663-3600; Email: leslieg@cals.arizona.edu

Authors

Ya-ming Xu − *Southwest Center for Natural Products Research, School of Natural Resources and the Environment, College of Agriculture and Life Sciences, University of Arizona, Tucson, Arizona 85706, United States*

Chandrashekhar Madasu − *Southwest Center for Natural Products Research, School of Natural Resources and the Environment, College of Agriculture and Life Sciences, University of Arizona, Tucson, Arizona 85706, United States*

Manping X. Liu − *Southwest Center for Natural Products Research, School of Natural Resources and the Environment, College of Agriculture and Life Sciences, University of Arizona, Tucson, Arizona 85706, United States*

E. M. Kithsiri Wijeratne − *Southwest Center for Natural Products Research, School of Natural Resources and the Environment, College of Agriculture and Life Sciences, University of Arizona, Tucson, Arizona 85706, United States*

David Dierig − *Guayule Research, Bridgestone Americas, Inc., Eloy, Arizona 85131, United States*

Bob White − *Guayule Research, Bridgestone Americas, Inc., Eloy, Arizona 85131, United States*

István Molnár − *Southwest Center for Natural Products Research, School of Natural Resources and the Environment, College of Agriculture and Life Sciences, University of Arizona, Tucson, Arizona 85706, United States*

Complete contact information is available at: https://pubs.acs.org/10.1021/acsomega.1c01714

Funding

This project was supported by the USDA-NIFA (grant # 2017-68005-26867; Dr. Kimberly Ogden, PI) and Hatch projects 1005072 and 1020652 to A.A.L.G and I.M. Any opinions, findings, conclusions, or recommendations expressed in this publication/work are those of the authors and do not necessarily reflect the view of the U.S. Department of Agriculture. We thank Dr. Lijiang Xuan, Shanghai Institute of Material Medica, Chinese Academy of Sciences, P. R. China for HRMS data.

Notes

The authors declare the following competing financial interest(s): A.A.L.G. and I.M. have disclosed financial interests in Sun Pharma Advanced Research Co. Ltd., India (A.A.L.G.), Regulonix, LLC. USA (A.A.L.G.), Teva Pharmaceuticals Works Ltd., Hungary (I.M.) and the University of Debrecen, Hungary (I.M.) that are unrelated to the subject of the research presented here. All other authors declare no competing financial interests.

■ ABBREVIATIONS

ECD, electronic circular dichroism; EtOAc, ethyl acetate; HMBC, heteronuclear multibond correlation; HPLC, high-performance liquid chromatography; HRESIMS, high-resolution electrospray ionization mass spectroscopy; HSQC, heteronuclear single quantum coherence; MS, mass spectroscopy; MTT, 3-(4,5-dimethylthiazol-2-yl)-2,5-diphenyltetrazolium bromide; NMR, nuclear magnetic resonance; NOESY, nuclear Overhauser effect spectroscopy; NP, normal phase; PDA, photodiode array; RP, reverse phase; TLC, thin-layer chromatography; UV, ultraviolet

■ REFERENCES

(1) McGinnies, W. G.; Haase, E. F. Guayule: a rubber-producing shrub for arid and semiarid regions. *Office of Arid Lands Studies*; University of Arizona: Tucson Arizona, 1975.

(2) Rasutis, D.; Soratana, K.; McMahan, C.; Landis, A. E. A sustainability review of domestic rubber from the guayule plant. *Ind. Crops Prod.* **2015**, *70*, 383−394.

(3) (a) Schloman, W. W., Jr. Processing guayule for latex and bulk rubber. *Ind. Crops Prod.* **2005**, *22*, 41−47. (b) Pearson, C. H.; Cornish, K.; Rath, D. J. Extraction of natural rubber and resin from guayule using an accelerated solvent extractor. *Ind. Crops Prod.* **2013**, *43*, 506−510.

(4) (a) Snoeck, D.; Chapuset, T.; García García, J.; Sfeir, N.; Palu, S. Feasibility of a guayule commodity chain in the Mediterranean region. *Ind. Crops Prod.* **2015**, *75*, 159−164. (b) Jara, F. M.; Cornish, K.;

Carmona, M. Potential applications of guayulins to improve feasibility of guayule cultivation. *Agronomy* **2019**, *9*, 804.
(5) (a) Rodriguez-Hahn, L.; Romo de Vivar, A.; Ortega, A.; Aguilar, M.; Romo, J. Structures of argentatines A, B, and C from Parthenium argentatum. *Rev. Latinoam. Quim.* **1970**, *1*, 24−38. (b) Hernandez-Ortega, S.; Delgado, H. P.; Martínez, M. Incanilin (isoargentatin A) from Parthenium argentatum. *Acta Crystallogr., Sect. E: Struct. Rep. Online* **2005**, *61*, o1921−o1923.
(6) Romo, J.; Romo de Vivar, A.; Ortega, A.; Diaz, E. Guayulines A and B, new sesquiterpenes from Partherium argentatum. *Rev. Latinoam. Quim.* **1970**, *1*, 132−135.
(7) (a) Komoroski, R. A.; Gregg, E. C.; Shockcor, J. P.; Geckle, J. M. Identification of guayule triterpenes by two-dimensional and multi-pulse NMR techniques. *Magn. Reson. Chem.* **1986**, *24*, 534−543. (b) de Vivar, A. R.; Martínez-Vázquez, M.; Matsubara, C.; Pérez-Sánchez, G.; Joseph-Nathan, P. Triterpenes in Parthenium argentatum, structures of argtntatins C and D. *Phytochemistry* **1990**, *29*, 915−918.
(8) Maatooq, G. T.; El Gamal, A. A. H.; Furbacher, T. R.; Cornuelle, T. L.; Hoffmann, J. J. Triterpenoids from Parthenium argentatum x P. tomentosa. *Phytochemistry* **2002**, *60*, 755−760.
(9) Maatooq, G. T.; Hoffmann, J. J. Pyridine Alkaloids From A Parthenium Hybrid. *Z. Naturforsch., A: Phys. Sci.* **2002**, *57*, 211−215.
(10) Schloman, W. W., Jr.; Hively, R. A.; Krishen, A.; Andrews, A. M. Guayule byproduct evaluation: extract characterization. *J. Agric. Food Chem.* **1983**, *31*, 873−876.
(11) Bultman, J. D.; Gilbertson, R. L.; Adaskaveg, J.; Amburgey, T. L.; Parikh, S. V.; Bailey, C. A. The efficacy of guayule resin as a pesticide. *Bioresour. Technol.* **1991**, *35*, 197−201.
(12) Gutiérrez, C.; Gonzalez-Coloma, A.; Hoffmann, J. J. Antifeedant properties of natural products from Parthenium argentatum, P. argentatum×P. tomentosum (Asteraceae) and Castela emoryi (Simaroubeaceae) against Reticulitermes flavipes. *Ind. Crops Prod.* **1999**, *10*, 35−40.
(13) (a) Parra-Delgado, H.; García-Pillado, F.; Sordo, M.; Ramírez-Apan, T.; Martínez-Vázquez, M.; Ostrosky-Wegman, P. Evaluation of the cytotoxicity, cytostaticity and genotoxicity of argentatins A and B from Parthenium argentatum (Gray). *Life Sci.* **2005**, *77*, 2855−2865. (b) Flores-Rosete, G.; Martínez-Vázquez, M. Anti-inflammatory and cytotoxic cycloartanes from guayule (Parthenium argentatum). *Nat. Prod. Commun.* **2008**, *3*, 413−422. (c) Romero-Benavides, J. C.; Bailon-Moscoso, N.; Parra-Delgado, H.; Ramirez, M. I.; Villacis, J.; Cabrera, H.; Gonzalez-Arevalo, G.; Cueva, R.; Zentella-Dehesa, A.; Ratovitski, E. A.; Martínez-Vázquez, M. Argentatin B derivatives induce cell cycle arrest and DNA damage in human colon cancer cells through p73/p53 regulation. *Med. Chem. Res.* **2018**, *27*, 834−843.
(14) Martínez-Vázquez, M.; Martínez, R.; Perez, G. E.; Diaz, M.; Sanchez, M. H. Antimicrobial properties of argentatine A, isolated from Parthenium argentatum. *Fitoterapia* **1994**, *65*, 371−372.
(15) Tavarez-Santamaría, Z.; Jacobo-Herrera, N. J.; Rocha-Zavaleta, L.; Zentella-Dehesa, A.; Couder-García, B. d. C.; Martínez-Vázquez, M. A higher frequency administration of the nontoxic cycloartane-type triterpene argentatin A improved its anti-tumor activity. *Molecules* **2020**, *25*, 1780.
(16) Ray, D. T.; Dierig, D. A.; Thompson, A. E.; Coffelt, T. A. Registration of six guayule germplasms with high yielding ability. *Crop Sci.* **1999**, *39*, 300.
(17) Wijeratne, E. M. K.; Bashyal, B. P.; Liu, M. X.; Rocha, D. D.; Gunaherath, G. M. K. B.; U'Ren, J. M.; Gunatilaka, M. K.; Arnold, A. E.; Whitesell, L.; Gunatilaka, A. A. L. Geopyxins A-E, ent-Kaurane Diterpenoids from Endolichenic Fungal Strains Geopyxis aff. majalis and Geopyxis sp. AZ0066: Structure-Activity Relationships of Geopyxins and Their Analogues. *J. Nat. Prod.* **2012**, *75*, 361−369.
(18) Kholzineva, L. A.; Savina, A. A.; Mal'donado, I. R.; Shchavlinskii, A. N.; Pimenova, M. E. Triterpene glycosides of Astragalus quisqualis. I. The structure of quisquagenin. *Chem. Nat. Compd.* **1987**, *23*, 439−443.
(19) Parodi, F. J. "Structure elucidation of natural products from Asteraceae by modern NMR techniques and biomimetic transformations of 11,13-dihydroparthenolide.". LSU Historical Dissertations and Theses. 4528; Louisiana State University and Agricultural & Mechanical College, 1988. http://digitalcommons.lsu.edu/gradschool_disstheses/4528.
(20) Ganenko, T. V.; Isaev, M. I.; Gorovits, M. B.; Abdullaev, N. D.; Lutskii, V. I.; Semenov, A. A.; Abubakirov, N. K. Triterpene glycosides and their genins fromThalictrum foetidum. II. The structure of cyclofoetigenin A. *Chem. Nat. Compd.* **1985**, *21*, 345−350.
(21) Maatooq, G. T. Microbiological and chemical transformations of argentatin B. *Z. Naturforsch., A: Phys. Sci.* **2003**, *58*, 249−255.
(22) Escobedo-Martínez, C.; Concepción Lozada, M.; Hernández-Ortega, S.; Villarreal, M. L.; Gnecco, D.; Enríquez, R. G.; Reynolds, W. 1 H and 13 C NMR characterization of new cycloartane triterpenes from Mangifera indica. *Magn. Reson. Chem.* **2012**, *50*, 52−57.
(23) Bhacca, N. S.; Giannini, D. D.; Jankowski, W. S.; Wolff, M. E. Substituent effects in carbon-13 nuclear magnetic resonance spectroscopy. Progesterone, deoxycorticosterone, corticosterone, cortisol, and related steroids. *J. Am. Chem. Soc.* **1973**, *95*, 8421−8426.
(24) (a) Su, B.-N.; Park, E. J.; Mbwambo, Z. H.; Santarsiero, B. D.; Mesecar, A. D.; Fong, H. H. S.; Pezzuto, J. M.; Kinghorn, A. D. New Chemical Constituents of Euphorbia quinquecostata and Absolute Configuration Assignment by a Convenient Mosher Ester Procedure Carried Out in NMR Tubes. *J. Nat. Prod.* **2002**, *65*, 1278−1282. (b) Seco, J. M.; Quiñoá, E.; Riguera, R. The Assignment of Absolute Configuration by NMR†. *Chem. Rev.* **2004**, *104*, 17−118. (c) Gao, S.; Xu, Y.-m.; Valeriote, F. A.; Gunatilaka, A. A. L. Pierreiones A−D, Solid Tumor Selective Pyranoisoflavones and Other Cytotoxic Constituents fromAntheroporum pierrei. *J. Nat. Prod.* **2011**, *74*, 852−856. (d) Xu, Y.-m.; Mafezoli, J.; Oliveira, M. C. F.; U'Ren, J. M.; Arnold, A. E.; Gunatilaka, A. A. L. Anteaglonialides A-F and Palmarumycins CE1-CE3 from Anteaglonium sp. FL0768, a Fungal Endophyte of the Spikemoss Selaginella arenicola. *J. Nat. Prod.* **2015**, *78*, 2738−2747.
(25) (a) Reich, H. J.; Jautelat, M.; Messe, M. T.; Weigert, F. J.; Roberts, J. D. Nuclear magnetic resonance spectroscopy. Carbon-13 spectra of steroids. *J. Am. Chem. Soc.* **1969**, *91*, 7445−7454. (b) Martínez, M.; Flores, G.; de Vivar, A. R.; Reynolds, G.; Rodriguez, E. Guayulins C and D from guayule (Parthenium argentatum). *J. Nat. Prod.* **1986**, *49*, 1102−1103.
(26) Wheeler, O. H.; Mateos, J. L. Reactivity Studies on Natural Products: v. Rates of Borohydride Reduction of Some Ring a and B Steroid Ketones. *Can. J. Chem.* **1958**, *36*, 1049−1052.
(27) Romo de Vivar, A.; Guerrero, C.; Wittgreen, G. Terpenoids from Parthenium incanum H.B.K. *Rev. Latinoam. Quim.* **1970**, *1*, 39−43.

https://doi.org/10.1021/acsomega.1c01714
ACS Omega 2021, 6, 15486−15498